Food Chemistry: X 27 (2025) 102427

Contents lists available at ScienceDirect

Food Chemistry: X

journal homepage: www.sciencedirect.com/journal/food-chemistry-x

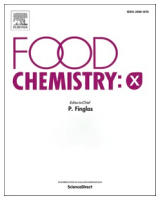

Study on taste release and perception mechanism of japonica rice during oral processing

Sailimuhan Asimi [c], Zhang Min [a,b,*]

[a] Beijing Advanced Innovation Center for Food Nutrition and Human Health, Beijing Technology and Business University, Beijing 100048, China
[b] Beijing Engineering and Technology Research Center of Food Additives, Beijing Technology and Business University, 11 Fucheng Road, Beijing 100048, China
[c] School of Public Health, Xinjiang Medical University, Urumqi 830011, China

ARTICLE INFO

Keywords:
Japonica rice
Taste
Oral processing
Perception

ABSTRACT

The sensorial experience of japonica rice is a critical factor that profoundly influences consumer choice. Despite this, the mechanisms underlying the release and perception of flavors during the oral processing of japonica rice are still not clearly understood. To address this gap, we conducted an in-depth investigation into the flavor release and gustatory perception dynamics of japonica rice during mastication using high-performance liquid chromatography (HPLC) and molecular docking simulations. Our findings revealed that umami taste was predominant during the initial stages of oral processing, whereas sweetness emerged as the dominant flavor in the subsequent phases. Moreover, we identified 16 key taste-active compounds that are released during the oral processing of japonica rice. Utilizing partial least squares regression (PLSR) analysis, we observed that glucose, sucrose, proline, maltose, and fructose were positively and significantly associated with the perception of sweetness in japonica rice. Concurrently, aspartic acid and glutamic acid contributed to the enhancement of umami perception, while concurrently diminishing the perception of sweetness and sourness. Further molecular docking studies demonstrated that glucose and sucrose interact with the amino acid residues of the sweet taste receptors T1R2/T1R3, engaging in hydrogen bonding and hydrophobic interactions. These interactions potentiate the activity of T1R2/T1R3, thereby facilitating the detection of sweetness. Similarly, aspartic acid and glutamic acid bind to the amino acid residues of the umami receptors T1R1/T1R3, establishing hydrogen bonds and hydrophobic interactions. This binding enhances the activity of T1R1/T1R3, leading to an augmented perception of umami.

1. Introduction

Rice serves as the main dietary staple for half of the world's population (Zhu, Cheng, Zhang, et al., 2019). As living standards improve, there is a growing emphasis on the flavor quality of rice. Flavor quality refers to the overall sensory experience perceived when consuming rice, encompassing attributes such as taste, aroma, and texture (Asimi, Ren, Zhang, et al., 2022a, 2022b). Evaluation of sensory aspects is typically conducted based on national standards to assess rice flavor. However, conventional sensory studies in food often overlook the significant roles of saliva and chewing in oral processing and sensory perception, equating mouth-tasted sensory properties with intrinsic food characteristics. Furthermore, the interplay between odor and taste is greatly influenced by the structural properties of the food matrix, which are closely linked to its texture (Saint-Eve, Panouillé, Capitaine, et al., 2015). Consequently, traditional sensory research segregates food sensory characteristics such as aroma, taste, and texture, neglecting the impact of solid particle breakdown and specific surface area expansion during oral processing on the release rate and intensity of flavor molecules (Chen, 2015).

Food oral processing is a complex procedure involving ingestion, mastication, intermittent saliva secretion, oral bolus formation, swallowing, residual taste perception, and more (Chen, 2015). During oral processing, food is mechanically broken down through chewing and crushing, while saliva aids in the transmission of taste compounds within the food matrix to taste bud cells. This interaction triggers taste receptors, initiating the ion channel pathway of taste reception and leading to taste perception (Dengyong & Zhenxia, 2020).As the main

* Corresponding author at: Beijing Advanced Innovation Center for Food Nutrition and Human Health, Beijing Technology and Business University, Beijing 100048, China
E-mail address: zmin@th.btbu.edu.cn (Z. Min).

https://doi.org/10.1016/j.fochx.2025.102427
Received 5 May 2024; Received in revised form 29 March 2025; Accepted 31 March 2025
Available online 1 April 2025

component of rice, starch is hydrolyzed by salivary α-amylase in the oral processing of rice, which plays an essential role in the taste and texture of rice. Amylopectin also easily reacts with salivary amylase in the mouth and decomposes into maltose, bringing sweetness (Ong & Blanshard, 1995). Therefore, taste largely determines consumers' preferences. In addition, in the oral processing of food, the main taste substances, such as reducing sugars, nucleotides, and free amino acids, also impact food taste. Meanwhile, bolus's texture properties and moisture content affect the release of salty/umami flavors (Deng, 2017). The detection methods of taste substances include HPLC, HPLC-MS, amino acid analyzer, etc.(Pionnier, Net, et al., 2004). Pu et al. (Pu et al., 2020) used HPLC to analyze taste substances in the oral processing of bread. It was found that malic acid, succinic acid, sodium chloride, valine, and sucrose are the key taste substances in the oral processing of bread. Deng (2017) used the HPLC method to analyze braised pork's flavor amino acids and nucleotides during oral processing. The results showed that flavor nucleotides and umami amino acids' content significantly negatively correlated with their fat content. Liu et al. (Dongxiao, 2021) analyzed the reducing sugars in the oral processing of indica rice by HPLC. They found that sucrose, maltose, and fructose were the key taste substances related to sweetness in the oral processing of indica rice. In the process of oral processing, dynamic sensory evaluation of temporal dominance of sensations (TDS) and D-QDA are important sensory analysis methods for studying the oral processing of food (Saint-Eve et al., 2015). This analytical method has been used in food oral processing studies of dairy products (Nguyen, Bhandari, & Prakash, 2016) and bread (Dandan, Huiying, Yuyu, et al., 2019). Pu et al. (Pu, 2020) used these two methods to determine that sourness, umami, and sweetness are the taste perceptions in the oral processing of bread.

During oral processing, taste substances are transferred to taste bud cells via saliva, combine with taste receptors (TRCs), are transmitted through specific ion channels, and processed and fed back to the brain to produce flavor perception. Taste receptor T1R (taste receptor type 1 member) consists of three subunits, T1R1, T1R2, and T1R3, which can further dimerize to form sweet taste receptors (T1R2/T1R3) and umami taste receptors (T1R1/T1R3)(Liu, Da, & Liu, 2019). Among them, T1R2/T1R3 is a taste receptor with a high affinity for various sweet substances, which can recognize a variety of sweet tastes, including simple sugars, different artificial sweeteners, D-amino acids, and high-intensity sweet proteins. T1R2/T1R3 Sweet-sensing taste receptors combine with sugars such as sucrose to activate α-flavoring, thereby activating adenylyl cyclase (AC) to produce cAMP (3′, 5′-cyclic adenylate), increasing intracellular cAMP concentration, and cAMP directly activates protein kinase A (PKA), causing phosphorylation of K+ channels, resulting in the closure of ion channels, inhibiting K+ efflux, causing membrane depolarization and neurotransmitter release to perceive sweetness (Nelson, Hoon, Chandrashekar, et al., 2001). In addition, T1R1/T1R3 are taste receptors for umami perception. T1R1/T1R3 can recognize umami substances, including glutamic acid, umami peptides with a molecular weight of less than 3000 Da, etc. (Lapis, Penner, & Lim, 2016). The umami substance binds to T1R1/T1R3, activates PLC-b2, produces DAG and IP3, and IP3 binds to IP3R3 so that the intracellular Ca^{2+} is released, which activates the TRPM5 channel, and Na^{+} flows into the cell, which eventually leads to membrane depolarization, and neurotransmitter release. In addition, mGluR4 is also an umami receptor, mainly expressed in the TRCs of the delineated papilla and phyllodes papilla of the tongue, resulting in umami perception (Liu et al., 2019).

The food bolus prepared in vitro simulated oral processing model was used as the research object. The taste substances such as amino acids, reducing sugars, glucose, maltose, nucleotides, and organic acids were quantitatively analyzed by high-performance liquid chromatography. Through correlation analysis and combined with Taste active value (TAV) and taste sensory evaluation results, the compounds that contribute to taste perception in the oral processing of japonica rice were identified. The taste perception of japonica rice during oral processing was further analyzed by two dynamic sensory evaluation methods, TDS and D-QDA. Based on the key taste substances identified in the oral processing of japonica rice, the protein structure of taste receptors was evaluated by the protein structure modeling tool (SWISS-MODEL Tools), and the rationality of the protein structure was further confirmed by the Laplace diagram. Molecular docking of receptor protein and flavor ligand was carried out by Auto Dock Vina software. The binding site and binding method of receptor and ligand were determined by affinity (kcal/mol) to explore the human perception mechanism of japonica rice flavor. The results of this study provides important theoretical support for global food security, food science and healthy diet. The results not only optimize japonica rice varieties and processing technology, promote cross-cultural food consumption and sustainable development, but also lay a solid scientific foundation for rice improvement, processing technology upgrading, food safety and nutrition guidelines formulation and food industry innovation.

2. Material and methods

2.1. Materials and reagents

2.1.1. Materials

Kenyu 38 (KY-38) was transplanted by machine in mid-to-late May 2019, with plant row spacing of 15 × 30 cm and 3 to 4 seedlings per hole. The whole growth period of pure nitrogen was 15–17 kg/ mu, the rice growth period was 163 days and rice moisture reached about 16 % with a harvester. The sowing and transplanting of KY-38 grain seeds took place in the summer of 2019 at the Binhai Agricultural Research Institute of Hebei Academy of Agriculture and Forestry Sciences experimental field. The growth, fertilization, and management of the rice were consistent. The rice grain underwent ridging and grinding processes using a practical ridging machine (THU35C, SATAKE, Suzhou, China) and a rice milling machine (TM05C, SATAKE, Suzhou, China).

2.1.2. Reagents

Food-grade sucrose, sodium chloride , citric acid, quinine and sodium glutamate are available from Shanghai Sugar & Tobacco Group Co., LTD. Chromatographic pure 5′ -cytidine (5'-CMP), 5′ -guanylate (5'-GMP), 5′ -inosinic acid (5'-IMP), 5′ -adenylate (5'-AMP), EDTA calcium disodium (EDTA calcium salt) are purchased from Sigma-Aldrich; Chromatographic pure tartaric acid, pyruvate, malic acid, ascorbic acid, lactic acid, citric acid, pyroglutamic acid, fumarate, succinic acid, sulfosalicylic acid, potassium dihydrogen phosphate, and phosphoric acid are available from Sinophurt Chemical Reagent Beijing Co., LTD.

2.2. Preparation of cooked rice

The rice was cooked according to Asimi et al.(Asimi, Xin, Min, et al., 2022). Briefly, weighted 200.0 g rice and added 240.0 g water soaked for 30 min at room temperature, then cook for 30 min and braised with heat preservation for 15 min in an electric steamer (ZN28YK807–150, 10 L, SUPOR, Suzhou, China). After the rice is steamed, weigh 10.0 ± 0.1 g of rice balls, wrap them with plastic film rice balls, and put them into a hot steam storage tank. During the evaluation, the temperature of the storage tank should be kept between 40 and 50 °C.

2.3. Sensory evaluation

Sensory evaluation tests were conducted in accordance with the Helsinki Declaration, utilizing TDS and D-QDA methods to evaluate taste perception during cooked rice oral processing. D-QDA evaluation is carried out according to Oliver, Cicerale, Pang, and Keast (2018) and Pu Dandan (Pu, 2020) method, which is divided into three steps: selection of evaluators, training, and experiment.

2.3.1. The selection of sensory evaluators

Sensory evaluators were selected according to our previous research methods Asimi et al. (Asimi et al., 2022). Briefly, 10 healthy adults (5 women and 5 men (age range 18–25 years) with normal occlusal teeth were selected from 30 healthy adults (age 18–25) based on their salivary flow rates and oral processing speeds. In our previous study by Liu et al. (2020), the dynamic measurement of salivary flow rate (Sf) was achieved by calculating saliva secretion (SA) as the difference between the moisture content of the food bolus and the original rice moisture, assessed through a drying method. Sf was computed as the ratio of SA to chewing count (Nc), indicating the average secretion per chew. Evaluators utilized handheld timers and tactile counters to record oral processing time (Tc) and Nc. Participants exhibiting extreme salivary flow rates (top and bottom 10 %) and oral processing speeds (fastest and slowest 10 %) were excluded from the study. Additionally, those with salivary flow rates outside the normal range ($<$20 mg/s or $>$ 30 mg/s) and individuals with chewing durations beyond the acceptable limits ($<$16 s or $>$ 26 s) were also excluded to minimize variability in saliva secretion calculations, based on pilot study analyses. All selected participants were healthy, possessed natural teeth, had no significant dental issues or dentures, and were not undergoing any medication that could influence muscle function or salivary flow. The study protocol was approved by the Ethics Review Committee of China Agricultural University, the study subjects signed written informed consent before the start of the study, and all 10 evaluators completed the study.

2.3.2. Training of sensory evaluators

Evaluators participated in a two-alternative forced-choice (2-AFC) test, adhering to ISO 5495 standards. They were presented with food-grade and pharmaceutical-grade solutions, which included glucose (50.00 g/L and 10.00 g/L), citric acid (5.00 g/L and 1.00 g/L), sodium chloride (15.00 g/L and 3.00 g/L), sodium glutamate (20.00 g/L and 4.00 g/L), and quinine (6.00 mg/L and 1.20 g/L), each marked with distinct three-digit codes. A dropper was used to deliver 2 mL of each solution, which varied in concentration but contained the same solute, directly into the evaluators' mouths. The evaluators were tasked with identifying the solution that displayed greater taste intensity, with only those achieving 100 % accuracy selected for further analysis.

2.3.3. Sensory evaluation experiment

Ten evaluators underwent four weeks of ranking test training, with 20-min sessions occurring twice weekly. Taste solutions included glucose (50.00 g/L), citric acid (5.00 g/L), sodium chloride (15.00 g/L), sodium glutamate (20.00 g/L), and quinine (6.00 mg/L), diluted serially at ratios of 1:2, 1:4, 1:6, 1:8, and 1:16. Evaluators ranked five concentrations based on perceived taste intensity. After training, evaluators recorded taste descriptors during cooked rice oral processing. Chewing duration (22 s) and blocking intervals (6 and 22 s) followed Asimi et al. (2022).According to the Pu Dandan, Zhang, Sun, et al. (2020), methods, for D-QDA analysis, evaluators rated sour, sweet, and salty taste intensity on a 1–9 scale (1: weak, 5: medium, 9: strong) during rice oral processing. For sweetness, sucrose is the reference compound, with intensity levels at concentrations of 30 g/L (9 points), 9.38 g/L (5 points), and 3 g/L (1 point).Citric acid is used as the reference for sourness, with intensity levels set at 2.50 g/L (9 points), 1 g/L (5 points), and 0.30 g/L (1 point).For saltiness, sodium chloride serves as the reference compound, with intensity levels corresponding to 7.500 g/L (9 points), 2.81 g/L (5 points), and 1.00 g/L (1 point).In TDS analysis, they identified the dominant taste attribute during each blocking time. To enhance operability and reproducibility, oral processing times (6, 12, 18, 22 s) were converted to chewing durations (10, 20, 30, 35 s) based on a 1.59 Hz chewing frequency (Asimi et al., 2022). Additional chewing times (5, 15, 25 s) enriched the data set. All evaluators underwent four weeks of training, with each session lasting 40 min and held weekly, prior to the TDS experiment. Each experiment was conducted in triplicate.

The D-QDA curve of taste perception was drawn according to the intensity changes of different taste attributes over time. The TDS evaluation of flavor required the evaluators to select the dominant flavor properties (sweet, sour, and umami) at 5, 10, 15, 20, 25, 30, and 35 chews of the rice. The taste perception TDS curve is drawn by statistical probability. TDS, the results of the analysis according to the random selection probability P and significantly higher than that of random selection probability P0, its calculation according to the formula 1 and 2.

$$P = 1/(1+s) \tag{1}$$

$$Po = P + 1.645 \times \sqrt{P(1-P)} \Big/ \sqrt{n \times r} \tag{2}$$

In formulas 1–1 and 1–2, s represents the number of sensory attributes of taste; n indicates the number of evaluators; r is the number of repetitions.

2.4. Methods of in vitro mastication

2.4.1. Stimulated saliva fluid

Stimulated saliva fluid (SSF) was prepared freshly before use according to Asimi et al. (Asimi et al., 2022) with the following concentration of salts: sodium chloride 6.8 mM, potassium chloride 5.4 mM, calcium chloride 5.4 mM, Sodium dihydrogen phosphate 6.5 mM, Sodium sulfide 0.1 mM, urea 16.7 mM, Carboxymethyl cellulose 12.4 mM. The pH was adjusted to 7.0 with 6 M HCl.

2.4.2. In vitro mastication

Rice bolus was prepared according to the previous research method in our laboratory: a method to simulate the oral processing of rice (Asimi et al., 2022; Asimi, Ren, Zhang, et al., 2021). First, add 75 U/mL α-amylase to SSF and preheat at 37 °C for 10 min. Second, 100 g of the cooked rice was mixed with 15.0 g SSF and then blended in a household blender (MJ-LZ20 Easy 201 A, Midea, Shanghai, China) for 0, 4 s, 8 s, 14 s, and 20 s. Following the simulated mastication step, each bolus was immediately used for taste properties measurement.

2.5. Methods for the determination of taste substances

2.5.1. Electronic tongue analysis

After 50 g of rice pellets prepared in Step 2.4.2 were collected and weighed immediately, 200 mL of 40 °C distilled water was added for homogenization (8000 r/min, 3 × 20 s) and centrifuged at 4 °C (3000 r/min, 10 min) to obtain the supernatant and filtrate with three layers of cloth for 3 times until the filtrate returned to room temperature. The electronic tongue (SA-402B, INSENT, Japan) was used for testing. Four cycles were performed for each sample, and the results of the last three measurements were taken after the first cycle was removed. The sensor response was stable and reproducible, and the data was valid.

2.5.2. Determination of reducing sugar

Collect and weigh the rice pellets prepared in Step 2.4.2. First, freeze immediately with liquid nitrogen to prevent further decomposition of the rice pellets by salivating enzymes. Then vacuum freeze-drying was carried out (Christ Alpha 1–2 LDplus, −80 °C, 0.01 mbar, 48 h), and the samples of freeze-dried food pellets were weighed and pulverized with a pulverizer (Retsch GM200, 15,000 rpm, 2 min) to achieve $<$100 μm particle size (verified by laser diffraction; Mastersizer 3000) for use. Chinese national standard methods GB 5009.8–2016 (China, 2016) detected glucose, sucrose, fructose, and maltose with modifications: (1) internal standard (allose, 10 μg/mL) added prior to extraction; (2) HPLC separation on Aminex HPX-87C column (Bio-Rad) at 85 °C.

2.5.3. Determination of organic acid in bolus

According to the method of Pu Dandan (Pu, 2020), nine organic acids were detected by high-performance liquid chromatography (CBM – 20 A, Shimazu Kitoya Consumables Co., Japan). Sample pretreatment was

consistent with 2.5.2 reducing sugar determination. 4 g of dry powder sample was taken, and 15 mL of pure water was added. After the vortex for 30 s, ultrasonic extraction was performed for 30 min (10 °C). After centrifugation (10,000 r/min, 10 min), the supernatant was filled to 10 mL with purified water, and 1 mL was added with 0.5 mL perchloric acid (8 %) for protein removal. After centrifugation (10,000 r/min, 10 min), the supernatant was passed through a nylon filter membrane (0.22 μm). Sample 1 mL of supernatant for analysis. The analysis method was referred to in the literature (Pu et al., 2020), and the experiment was repeated three times. HPLC analyzed 9 kinds of organic acids. The experiment was repeated three times.

Determination conditions: MP C18 (2) (4.6 mm × 250 mm × 5 μm) column, column temperature 30 °C; Mobile phase A (0.01 mol/L potassium dihydrogen phosphate, pH = 2.8 adjusted by 1 mol/L phosphoric acid), mobile phase B (methanol). Isometric elution (V A: V B, 98:2); Elution time 20 min; The flow rate was 1 mL/min. Injection volume 10 μL; The detection wavelength was 205 nm. Organic acids were quantitatively analyzed by the external standard method by gradient dilution of a mixed standard solution of organic acids in ultra-pure water.

Standard external methods carried out quantitative analysis of organic acids. Gradient dilution of tartaric acid, pyroglutamic acid, lactic acid, pyruvate, malic acid, citric acid, succinic acid, fumaric acid, ascorbic acid 0.001–0.1 g/L in the standard solution of mixed organic acids with ultra-pure water. With the concentration of organic acids as the horizontal coordinate and the corresponding peak area as the vertical coordinate, the standard curve of each organic acid was obtained.

2.5.4. Determination of taste nucleotides in bolus

Four flavor nucleotides (5'-ADP, 5'-AMP, 5'-IMP, 5'-GMP) were detected by high-performance liquid chromatography (CBM – 20 A, Shimadsu Kitaiyou Consumable Co., LTD., Japan) according to Deng Yajun's method (Deng, 2017).

Take a 4 g dry sample and add 15 mL water vortex for 30 s by ultrasonic extraction after 30 min (10 °C). After centrifugation (10,000 r/min, 10 min), the supernatant was filled to 10 mL with purified water, and 1 mL was added with 0.5 mL perchloric acid (8 %) for protein removal. After centrifugation (10,000 r/min, 10 min), the supernatant was passed through a nylon filter membrane (0.22 μm)—sample 1 mL of supernatant for analysis.

HPLC main technical parameters: MP C18 (2) (4.6 mm × 250 mm × 5 μm) column, column temperature: 30 °C, UV detector wavelength: 254 nm. Mobile phase A was methanol, and B was 0.05 mol/L potassium dihydrogen phosphate buffer solution (pH = 5.4). Binary mobile phase gradient (PDA) elution procedure: 0 min eluent A 0 %, eluent B 100 %, 11 min; At 12 min, it was adjusted to 10 % eluent A and 90 % eluent B for 6 min. At 18 min, eluent A was 2 %, eluent B was 98 %, and the detection was finished at 30 min. Flow rate: 0.8 mL /min; Sample size: 10 μL. Quantitative analysis of peak area.

Standard curve drawing: weigh 10 mg of each of four nucleotides (5'-ADP, 5'-AMP, 5'-IMP, 5'-GMP), dissolve them in ultra-pure water, and keep them at 10 mL at 4 °C for later use. Accurate absorption of four kinds of standard solution from 5 mL to 10 mL volumetric bottles, a fixed volume of ultra-pure water, to obtain a concentration of 500 μg/m L mixed standard solution. Then, the mixed standard solution with the concentration of 250, 100, 50, 25, 5, 2.5, 1, 0.5, and 0.1 μg/mL was diluted with ultra-pure water, which was used for HPLC detection. The standard curve regression equation was established with the concentration of each nucleotide as the abscissa (x) and the corresponding peak area A as the ordinate (y).

2.5.5. Determination of free amino acid content in bolus

According to Deng Yajun's method (Deng, 2017), 16 free amino acids were detected by an automatic amino acid analyzer (L8900, Hitachi High-Technologies, USA). First, take a 1.00 g sample, add 9 mL pure water, vortex for 30 s, ultrasonic extraction at 10 °C for 10 min, and centrifuge at low temperature (4 °C) for 10 min (10,000 r/m) to remove the supernatant. Next, 500 μL sulfosalicylic acid aqueous solution (50 %) was added to the supernatant, and 0.1 mol/L hydrochloric acid solution was incubated to 10 mL for 30 s and then centrifugated for 10 min (10,000 r/m). The supernatant was then passed through a nylon filter membrane (0.22 μm) for detection by an automatic amino acid analyzer.

2.5.6. Calculation of TAV

TAV reflects the contribution of a specific taste substance to the overall taste. If TAV is greater than 1, it indicates that the taste substance significantly impacts the taste of the sample, and the greater the value, the greater the contribution. TAV = concentration of taste substance/taste threshold of the substance.

2.5.7. Addition experiment

The key taste substances that contribute to the taste perception in the oral processing of japonica rice were verified by additive experiments. The key taste substances were added to the rice sample (10 g) according to the saliva dosage of 150 mg/g at different concentration gradients according to the concentration detected at different stages of oral processing. The rice sample and the aqueous solution were thoroughly mixed and then presented to the sensory evaluator. The contribution of the added taste substances to the rice was judged through the evaluation of the flavor profile of the rice, and the key taste substances were finally determined.

2.6. Data analysis

Microsoft Office 2016 and SPSS22 were used for statistical analysis, and all data were the average values of at least three measurements. PyMOL, Origin, Adobe Photoshop, and Adobe Illustrator were used to produce relevant graphics.

2.6.1. Taste receptor modeling

The taste receptor proteins T1R1, T1R2, and T1R3 are searched and collected in https://www.uniprot.org/, SWISS-MODEL tools (https://swissmodel.expasy.org/interactive) to MODEL protein sequences. Modeling results of homologous proteins, such as protein sequence similarity and coverage greater than 30 %, indicate that protein model structure prediction is reliable (Pu et al., 2020). Sweet taste receptor (T1R2/T1R3) and umami taste receptor (T1R1/T1R3) were obtained. Autodocktools-1.5.7 software was used for hydrogenation and electric core processing.

2.6.2. Molecular docking

The 3D structure PDB files of the key taste substances were searched and collected in the https://pubchem database. Use AutoDockTools-1.5.7 software for hydrogenation, electrification, and non-polar hydrogen treatment. Autodock Vina 1.5.7 was used for molecular docking, and affinity (kcal/mol) was used as the index to determine the relationship between receptor and ligand.

3. Results and discussion

3.1. Sensory evaluation

Based on D-QDA and TDS analysis, the changes in japonica rice taste profiles during chewing were observed (Fig.1. a). TDS results showed that sweetness was above the signature line in the oral processing of japonica rice. At the same time, sour and umami tastes were lower than the random line, indicating that sweetness was the main taste perception in the oral processing of japonica rice. Our research results are consistent with Pu Dandan (Pu, 2020), which found that sweetness is the main taste perception in bread oral processing. The umami flavor was dominant during chewing for 0–6 s, and after chewing for 7 s, the sweet flavor was dominant. The results of D-QDA (Fig.1. b) showed that the intensity of

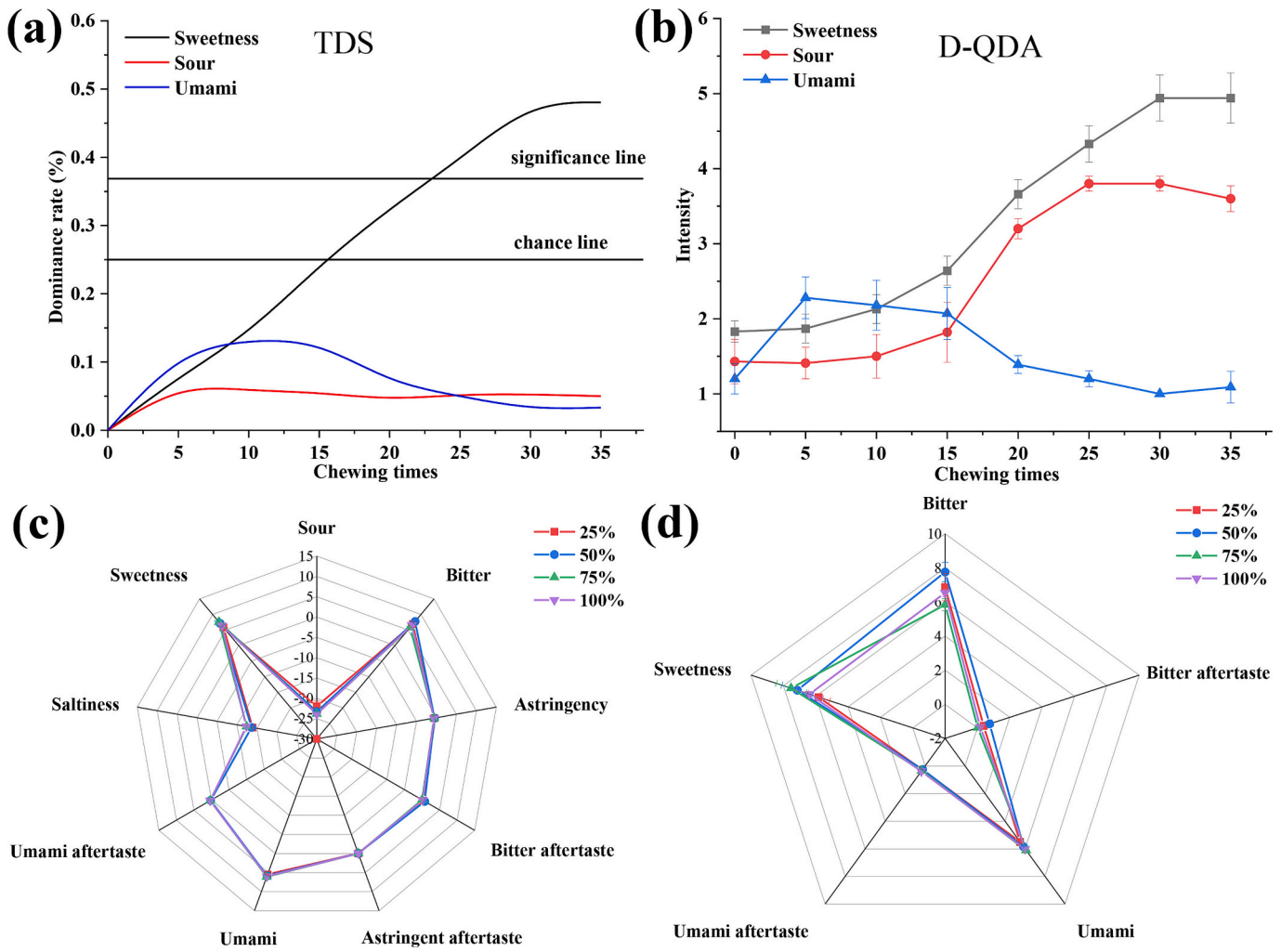

Fig. 1. (a) TDS curves of japonica rice during chewing. (b) Sensory evaluation results of the dynamic-quantitative descriptive analysis (D-QDA).c-d was electronic tongue taste analysis rice during chewing.

sweetness perception increased linearly during 0–18 s of chewing ($P<0.001$), and the intensity leveled off at chewing for 18–20 s. The trend of sweet taste perception was different from that of the D-QDA evaluation of bread in oral processing by Pu Dandan (Pu, 2020). The sweet taste perception of bread was significantly increased during 0–18 s oral processing. On the one hand, this difference may be caused by the different stages of oral processing of different foods. The time from ingestion to swallowing was 22 s for japonica rice and 18 s for bread (Pu, 2020). On the other hand, with the prolongation of the oral processing stage, saliva was continuously secreted, and the dilution of saliva led to the stable perception of the sweet taste of japonica rice at the later stage of chewing. The perceived intensity of the sour taste increased linearly during chewing 0–16 s ($P < 0.001$) and decreased gradually during chewing 16–22 s. The changing trend of sour taste perception is consistent with the changing direction of the sour taste of braised meat in oral processing evaluated by Dengyong et al. (2020) using time intensity and the gradual enhancement trend of a sour taste in bread oral processing tested by Pu Dandan (2020). The intensity of umami perception increased during 0–3 s chewing ($P < 0.001$), decreased gradually at 3–18 s, and leveled off at 18–22 s. The sweet substances are mainly derived from soluble sugar and sweet amino acids, which produce a precious perception of starch hydrolysis and a large amount of sugar in late chewing.

3.2. *Electronic tongue analysis*

As can be seen from Fig.1.c, in the oral chewing process of japonica rice, the astringency, sour taste, and saltiness of food pellets were below 0. Therefore, other tastes were used as effective evaluation indexes in pellets (Fig. 1.d.). In vitro oral chewing of japonica rice, there were significant differences in sweetness and umami taste. This is consistent with the results of TDS (Fig.1. a.) and D-QDA (Fig.1. b.) dynamic sensory evaluation.

As can be seen from Fig. 1.c, the umami flavor of japonica rice changed significantly during the oral process. In the oral processing process of japonica rice, the umami value was between 6.5 and 5.1 mV. From the 25 % to 75 % oral processing stage, the umami value of food pellets was significantly reduced (6.5–5.1), which may be related to saliva dilution. From the 75 % to 100 % oral processing stage, the change of the umami flavor of pellets tended to be stable. The variation of umami flavor in the late mastication period was consistent with Deng Yajun's research results (Deng, 2017). The observed increase in umami value during chewing can be attributed to the combined effects of physical disruption and enzymatic hydrolysis. As mastication physically disrupts the rice structure, the surface area of the food matrix increases, exposing starch granules to salivary α-amylase (Salles, Chagnon, Feron, et al., 2011). This enzyme hydrolyzes the exposed starch into maltose and dextrins, which not only reduces the viscosity of the food bolus but also releases bound umami compounds such as free glutamic acid

(Shiozawa, Kohyama, & Yanagisawa, 2010).

Sweetness is one of the most important taste characteristics of japonica rice. Fig. 1.d shows the changes in sweetness during oral processing of japonica rice simulated in vitro. In the simulated oral processing, the umami value of japonica rice varied significantly between 5.8 and 7.6 mV. From the 25 % to 75 % oral processing stage, the sweetness of pellets increased (5.8–7.5), aligning with Pu et al. (2020)'s observations on starch hydrolysis-driven sweetness release. This acceleration likely reflects progressive breakdown of amylopectin clusters (Shiozawa et al., 2010), increasing accessible sucrose and maltooligosaccharides. However, from the 75 % to 100 % oral processing stage, there was no significant difference in the umami taste of pellets, which suggesting sensory saturation or salivary dilution effects. This process is amplified in starch-rich foods due to prolonged oral processing, allowing sustained enzyme-substrate interaction. Mandel and Breslin (2012) demonstrated that individuals with high salivary amylase activity exhibit faster starch breakdown and elevated postprandial glucose levels, confirming its role in early digestion. Additionally, Stokes, Boehm, and Baier (2013) quantified the real-time degradation of starch during chewing using in-mouth models, linking enzymatic efficiency to mechanical fragmentation.

3.3. Soluble sugar analysis

The main component of japonica rice is starch. Some soluble sugar will be produced during chewing, which plays an important role in forming the taste of japonica rice. Salivary alpha-amylase is an *endo*-acting enzyme that catalyzes the hydrolysis of α-1,4 glycosidic bonds within the polymeric starch chain to produce short-chain sugars, including maltose, fructose, and glucose, which can induce different perceptions of sweetness in humans (Pu, 2020). Four kinds of water-soluble carbohydrates, including fructose, glucose, sucrose, and maltose, were detected in the simulated oral processing of japonica rice. The results of soluble sugar release during oral chewing of japonica rice are shown in Table 1. During the rice oral processing of japonica rice and, The average contents of fructose, glucose, sucrose, and maltose were 812.76 (15.47–1260.59) mg/100 g, 1467.79 (73.53–2550.15) mg/100 g, 389.31 (28.78–719.05) mg/100 g and 864.92 (11.13–1843.27) mg/kg, respectively. Glucose is the highest, followed by fructose, maltose, and sucrose. The content of reduced sugar in pellets increased significantly from 0 % to 25 % at the oral processing stage ($P < 0.05$) and slightly increased from 25 % to 50 % at the oral processing stage. Still, the difference was not significant ($P > 0.05$) and significantly increased from 50 % to 75 % at the oral oral ($P < 0.05$). From 75 % to 100 % oral mastication stage tended to be stable ($P > 0.05$). The increasing trend of glucose and sucrose was similar, and the expanding trend of fructose and maltose was identical. The variation trend of glucose during oral mastication of japonica rice in vitro was consistent with the study of bread by Pu Dandan et al. (Pu, 2020).

The taste characteristics of taste substances also depend on their taste threshold (Pu, 2020). To further explore the contribution of soluble sugars to taste in the oral processing of japonica rice, the results of taste analysis are shown in Table 1. The TAV of four kinds of soluble sugars were all higher, indicating that four kinds of reducing sugars were important compounds for perceiving sweetness in oral chewing of japonica rice. In the whole chewing stage, the TVA values of 4 reducing sugars were significantly increased ($P < 0.05$). Liu Dongxiao (2021) reported that sucrose, fructose, and maltose contributed to the sweetness of indica rice during oral processing, among which sucrose contributed the most to the sweetness. This is different from the results of this study. The possible reason is that different rice varieties present different tastes in oral processing.

3.4. Organic acid analysis

The release and flavor analysis results of 9 organic acids during oral processing of japonica rice are shown in Table 1. In the oral chewing process of japonica rice, the contents of organic acids in 0 %, 25 %, 50 %, 75 %, and 100 % pellets were 142.84 mg/100 g, 325.92 mg/100 g, 226.19 mg/100 g, 321.42 mg/100 g and 464.97 mg/100 g respectively. The concentration of succinic acid (7598–273.55 mg/100 g) was the highest, followed by pyruvate (11.23–82.11 mg/100 g) and tartaric acid (22.85–48.0 mg/100 g). By calculating the TAV values of organic acids, the TAV values of tartaric acid (0.63–1.17) and succinic acid (0.72–2.58) are more significant than 1, indicating that these two organic acids have important contributions to taste perception. These results were consistent with the Pudandan results (Pu, 2020), which indicated that tartaric acid and succinic acid had important effects on the taste perception of bread during oral chewing. Among them, tartaric acid significantly increased from 0 % to 25 % at the oral processing stage ($P < 0.05$), significantly decreased from 25 % to 50 % at the oral processing stage ($P < 0.05$), and significantly increased from 50 % to 100 % at the oral

Table 1
Release and taste analysis of taste compounds japonica rice in vitro mastication (mg/100 g).

Components	Threshold	0 %	TAV	25 %	TAV	50 %	TAV	75 %	TAV	100 %	TAV
Reducing sugar											
Fructose	90	15.47 ± 0.01^{d}	0.17	793.49 ± 0.09^{c}	8.82	866.70 ± 0.13^{c}	9.63	1260.59 ± 0.42^{a}	14.01	1127.58 ± 0.40^{a}	12.53
Glucose	110	73.53 ± 0.00^{d}	0.67	1138.19 ± 0.11^{c}	10.35	1266.56 ± 0.91^{c}	10.74	2310.50 ± 1.13^{a}	21	2550.15 ± 0.35^{a}	23.18
Sucrose	100	28.78 ± 0.01^{c}	0.29	260.18 ± 0.24^{b}	2.6	279.90 ± 0.40^{b}	2.8	658.62 ± 0.45^{a}	6.59	719.05 ± 0.15^{a}	7.19
Maltose	130	11.13 ± 0.01^{c}	0.08	226.99 ± 0.07^{b}	1.45	438.07 ± 1.26^{b}	3.17	1843.27 ± 1.49^{a}	7.95	1805.16 ± 0.31^{a}	14.71
Organic acids											
Tartaric acid	41	25.98 ± 0.00^{c}	0.63	34.62 ± 2.02^{b}	0.84	22.85 ± 1.47^{c}	0.56	38.14 ± 1.69^{b}	0.93	48.00 ± 1.21^{a}	1.17
Pyruvic acid	300	11.23 ± 0.95^{d}	0.04	71.82 ± 4.33^{a}	0.24	28.64 ± 1.32^{c}	0.1	60.66 ± 3.08^{b}	0.2	82.11 ± 0.73^{a}	0.27
Malic acid	500	10.72 ± 0.51^{b}	0.02	7.31 ± 0.63^{c}	0.01	10.36 ± 0.11^{b}	0.02	15.85 ± 0.11^{a}	0.03	17.40 ± 1.24^{a}	0.03
Ascorbic acid	120	3.38 ± 0.04^{a}	0.03	2.77 ± 0.03^{b}	0.02	2.57 ± 0.05^{b}	0.02	2.83 ± 0.06^{b}	0.02	3.85 ± 0.04^{a}	0.03
Lactic acid	260	0.67 ± 0.06^{b}	0	1.01 ± 0.02^{b}	0.01	0.28 ± 0.25^{b}	0	2.05 ± 0.74^{a}	0	2.25 ± 0.27^{a}	0.01
Citric acid	310	5.42 ± 0.90^{c}	0.02	9.21 ± 0.99^{b}	0.03	4.87 ± 0.42^{c}	0.02	8.23 ± 0.41^{b}	0.03	16.90 ± 1.15^{a}	0.05
Pyroglutamic acid	500	4.14 ± 0.26^{c}	0.01	7.05 ± 0.51^{b}	0.01	5.59 ± 0.61^{c}	0.01	7.85 ± 0.95^{b}	0.02	10.30 ± 0.58^{a}	0.02
Fumaric acid	400	5.30 ± 0.84^{b}	0.01	2.25 ± 0.09^{c}	0.01	3.24 ± 0.07^{c}	0.01	1.82 ± 0.09^{c}	0	10.62 ± 0.70^{a}	0.03
Succinic acid	106	75.98 ± 0.57^{c}	0.72	188.83 ± 7.19^{b}	1.78	147.78 ± 2.82^{b}	1.39	185.05 ± 5.65^{b}	1.75	273.55 ± 8.69^{a}	2.58
Nucleotides											
5'-CMP	ND	3.19 ± 0.08^{c}	–	20.39 ± 2.48^{ab}	–	24.25 ± 2.03^{ab}	–	16.82 ± 1.69^{b}	–	28.64 ± 0.85^{a}	–
5'-GMP	12.5	3.66 ± 0.07^{a}	0.29	1.36 ± 0.14^{b}	0.11	1.45 ± 0.08^{b}	0.12	0.81 ± 0.21^{c}	0.06	0.95 ± 0.03^{c}	0.08
5'-IMP	25	3.56 ± 0.08^{a}	0.14	1.00 ± 0.11^{b}	0.04	1.30 ± 0.05^{b}	0.05	0.90 ± 0.15^{c}	0.04	1.02 ± 0.10^{b}	0.04
5'-AMP	50	3.35 ± 0.77^{c}	0.07	21.83 ± 0.76^{b}	0.44	17.77 ± 0.52^{b}	0.36	23.12 ± 1.84^{b}	0.46	34.62 ± 2.31^{a}	0.69
Flavor nucleotide		10.56 ± 0.80^{c}		24.19 ± 0.71^{b}		20.52 ± 0.52^{b}		24.83 ± 1.49^{b}		36.60 ± 2.32^{a}	

Different letters in the same line indicate significant differences ($P < 0.05$); 5 '-CMP: 5' -cytidylate, 5 '-GMP: 5' -guanylate, 5 '-IMP: 5' -inosinic acid, 5 '-AMP: 5' -adenylate. The flavor nucleotides are the sum of 5'-IMP, 5′ -GMP, and 5'-AMP.

processing stage ($P < 0.05$). Succinic acid increased significantly from 0 % to 25 % at the oral processing stage ($P < 0.05$), had no significant difference from 50 % to 75 % at the oral processing stage ($P > 0.05$), and significantly increased from 75 % to 100 % at the oral processing stage ($P < 0.05$).

3.5. Nucleotides analysis

The release of flavor nucleotides and flavor analysis results during oral chewing of japonica rice are shown in Table 1. During the oral mastication of japonica rice, the nucleotide contents in the pellets at 0 %, 25 %, 50 %, 75 %, and 100 % oral mastication stages were 93.29 mg/100 g, 8.23 mg/100 g, 7.78 mg/100 g and 100.69 mg/100 g, respectively. Although the content of flavor nucleotides at the swallowing point was significantly higher than that of japonica rice ($P < 0.05$) (3 times higher), the average content of flavor nucleotides 5'-IMP was 1.56 mg/100 g in vitro simulated oral mastication, which was lower than the threshold (14 mg/100 g). Compared with japonica rice, 5'-IMP content decreased by 71.91 %, 63.48 %, 74.72 %, and 71.35 %, respectively, in the 25 %, 50 %, 75 %, and 100 % stages of oral chewing pellets. The reason is that mastication and crushing cause the change of pellet structure, which leads to the degradation of various nucleotides along with the enzymatic hydrolysis of saliva. It is also caused by entering flavor nucleotides into saliva and swallowing during oral mastication. By calculating the TAV value of nucleotides, it was found that four nucleotides did not contribute to the taste perception of japonica rice. In conclusion, the nucleotides of flavorful pellets in oral chewing of japonica rice did not contribute to taste perception. This finding is consistent with previous research on the role of nucleotides in taste perception. For instance, studies have shown that while nucleotides such as inosine 5′-monophosphate (IMP) and guanosine 5′-monophosphate (GMP) can enhance umami taste when present in sufficient concentrations, their contribution is minimal when their TAV values are below the perceptible threshold (Chen, Yang, Xiao, et al., 2023). In the context of japonica rice, our analysis revealed that the concentrations of these nucleotides were insufficient to reach the perceptible threshold, thus confirming their negligible impact on taste perception.

3.6. Free amino acid analysis

The release and flavor analysis results of 16 free amino acids during oral chewing of japonica rice are shown in Table 2. In the oral chewing process of japonica rice, the contents of free amino acids in the pellets at 0 %, 25 %, 50 %, 75 %, and 100 % oral processing stages were 10.39 mg/100 g, 13.97 mg/100 g, 12.73 mg/100 g, 18.36 mg/100 g and 18.46 mg/100 g, respectively. Among them, the amino acids of umami accounted for 15.87 %, 16.47 %, 15.47 %, 5.03 %, and 4.82 % of the total amino acids. From the 0 % to 25 % oral processing stage, the total amino acids of umami flavor significantly increased ($P < 0.05$); from the 25 % to 50 % oral processing stage, the total amino acids of umami flavor significantly decreased ($P < 0.05$), from 75 % to 100 % oral processing stage, the change of total amino acids of umami flavor tended to be stable. This result is consistent with the D-QDA and TDS dynamic sensory evaluation results. Sweet amino acids accounted for 46.83 %, 40.13 %, 35.33 %, 60.55 %, and 55.09 % of the total amino acids. From the 0 % to 50 % oral processing stage, sweet amino acids had no significant change ($P > 0.05$); from the 50 % to 75 % oral processing stage, sweet amino acids significantly increased ($P < 0.05$). From the 75 % to 100 % oral processing stage, the change of sweet amino acid totals pellets tended to be stable. Bitter amino acids accounted for 37.30 %, 43.41 %, 49.20 %, 34.42 %, and 40.09 % of the total amino acids. From the 0 % to 25 % oral processing stage, the total amount of bitter amino acids increased significantly ($P < 0.05$), while from the 25 % to 100 % oral processing stage, sweet amino acids had no significant change ($P > 0.05$). During simulated oral mastication in vitro, the content of bitter amino acids in the pellets increased, but there was no significant difference in each stage of oral mastication. The TAV values of free amino acids were calculated. The TAV values of 2 acidic amino acids (aspartic acid and glutamic acid), three sweet amino acids (glycine, alanine, and proline), and 5 bitter amino acids (valine, lysine, arginine, histidine, and methionine) were ≥ 1, indicating that the TAV values of free amino acids had a significant contribution to the taste of japonica rice.

3.7. Identification of key taste substance

3.7.1. Correlation analysis between taste substance and taste perception

PLSR was used to analyze the correlation between taste substance (TAV ≥ 1) and sensory attribute changes (D-QDA analysis) during oral chewing of japonica rice. The result is shown in Fig. 2. PLSR analysis results show that the cumulative Q^2 is 0.99 (>0.6), indicating that the analysis model of this data is reliable. The predictive variable of the first principal component was 63.5 %, the second principal component 20.4 %, and the third principal component 16.1 % (Fig. 2a-d).

The 25 % and 50 % stages of oral mastication are in the negative axis

Table 2
Release and taste analysis of free amino acids of rice in vitro mastication (mg/g).

Free amino acids		Threshold	0 %	TAV	25 %	TAV	50 %	TAV	75 %	TAV	100 %	TAV
Asp	umami	1.0	1.05 ± 0.33^{b}	1.05	1.70 ± 0.03^{a}	1.70	1.38 ± 0.03^{b}	1.38	0.80 ± 0.03^{c}	0.80	0.80 ± 0.03^{c}	0.80
Glu	umami	0.3	0.60 ± 0.01^{a}	2.00	0.60 ± 0.01^{a}	2.00	0.60 ± 0.01^{a}	2.00	0.13 ± 0.01^{b}	0.43	0.13 ± 0.01^{b}	0.43
UAA			1.65 ± 0.33^{b}	0.21	2.30 ± 0.03^{a}		1.98 ± 0.03^{b}		0.93 ± 0.03^{c}		0.93 ± 0.01^{c}	
Thr	sweet	2.6	0.44 ± 0.19^{a}	0.72	0.55 ± 0.02^{a}	0.21	0.41 ± 0.02^{a}	0.16	0.61 ± 0.02	0.23	0.61 ± 0.02	0.23
Ser	sweet	1.5	1.08 ± 0.35^{a}	0.85	1.08 ± 0.03^{a}	0.72	0.20 ± 0.01^{b}	0.13	0.21 ± 0.01^{b}	0.14	0.20 ± 0.01^{b}	0.13
Gly	sweet	1.3	0.90 ± 0.36^{b}	3.45	1.11 ± 0.04^{b}	0.85	1.43 ± 0.01^{a}	1.10	1.26 ± 0.12^{a}	0.97	1.74 ± 0.01^{a}	1.34
Ala	sweet	0.6	1.66 ± 0.51^{a}	0.21	2.07 ± 0.06^{a}	3.45	0.50 ± 0.01^{b}	0.83	0.49 ± 0.01^{b}	0.82	0.51 ± 0.01^{b}	0.84
Pro	sweet	3.0	0.80 ± 0.01^{c}	0.27	0.80 ± 0.01^{c}	0.27	1.99 ± 0.05^{b}	0.66	8.60 ± 0.02^{a}	2.87	7.58 ± 0.15^{a}	2.53
SAA			4.87 ± 0.89^{b}		5.61 ± 0.14^{b}		4.52 ± 0.04^{b}		11.16 ± 0.44^{a}		10.12 ± 0.16^{a}	
Val	bitter	0.4	0.93 ± 0.39^{b}	2.32	1.86 ± 0.02^{a}	4.65	1.55 ± 0.03^{a}	3.88	1.55 ± 0.03^{a}	3.86	1.60 ± 0.03^{a}	4.00
Lys	bitter	0.5	0.44 ± 0.11^{a}	0.88	0.57 ± 0.03^{a}	1.14	0.43 ± 0.01^{a}	0.85	0.46 ± 0.01^{a}	0.93	0.48 ± 0.01^{a}	0.96
Ile	bitter	0.9	0.06 ± 0.01^{b}	0.07	0.06 ± 0.01^{b}	0.07	0.06 ± 0.01^{b}	0.07	0.06 ± 0.01^{b}	0.07	0.27 ± 0.01^{a}	0.30
Leu	bitter	1.9	0.14 ± 0.01^{c}	0.07	0.61 ± 0.01^{b}	0.32	1.20 ± 0.02^{a}	0.63	0.17 ± 0.02^{c}	0.09	0.68 ± 0.01^{b}	0.36
Tyr	bitter	nd	0.25 ± 0.02^{b}	–	0.43 ± 0.02^{b}	–	0.85 ± 0.01^{a}	–	0.50 ± 0.02^{b}	–	0.90 ± 0.02^{a}	–
Phe	bitter	0.9	0.33 ± 0.01^{a}	0.36	0.56 ± 0.01^{a}	0.62	0.28 ± 0.01^{a}	0.31	0.62 ± 0.02^{a}	0.68	0.40 ± 0.01^{a}	0.45
His	bitter	0.2	1.06 ± 0.14^{a}	5.28	1.19 ± 0.03^{a}	5.97	1.34 ± 0.32^{a}	6.69	1.13 ± 0.04^{a}	5.64	1.58 ± 0.04^{a}	7.89
Arg	bitter	0.5	0.58 ± 0.02^{a}	1.17	0.67 ± 0.00^{a}	1.35	0.58 ± 0.03^{a}	1.16	0.71 ± 0.01^{a}	1.41	0.65 ± 0.01^{a}	1.30
Met	bitter	0.3	0.10 ± 0.00^{b}	0.33	0.10 ± 0.00^{b}	0.33	0.01 ± 0.00^{b}	0.03	1.15 ± 0.03^{a}	3.82	1.15 ± 0.03^{a}	3.82
BAA			3.88 ± 0.10^{b}		6.06 ± 0.02^{a}		6.30 ± 0.16^{a}		6.34 ± 0.10^{a}		7.73 ± 0.13^{a}	
FAA			10.39 ± 0.10^{c}		13.97 ± 0.31^{b}		12.73 ± 0.26^{b}		18.36 ± 0.56^{a}		18.46 ± 0.26^{a}	

Different letters in the same line indicate significant differences ($P < 0.05$); UAA: umami amino acid; SAA, sweet amino acid; BAA, bitter amino acid; FAA: Free amino acids (sum). UAA: umami amino acid; SAA, sweet amino acid; BAA, bitter amino acid; FAA: Free amino acids (sum).

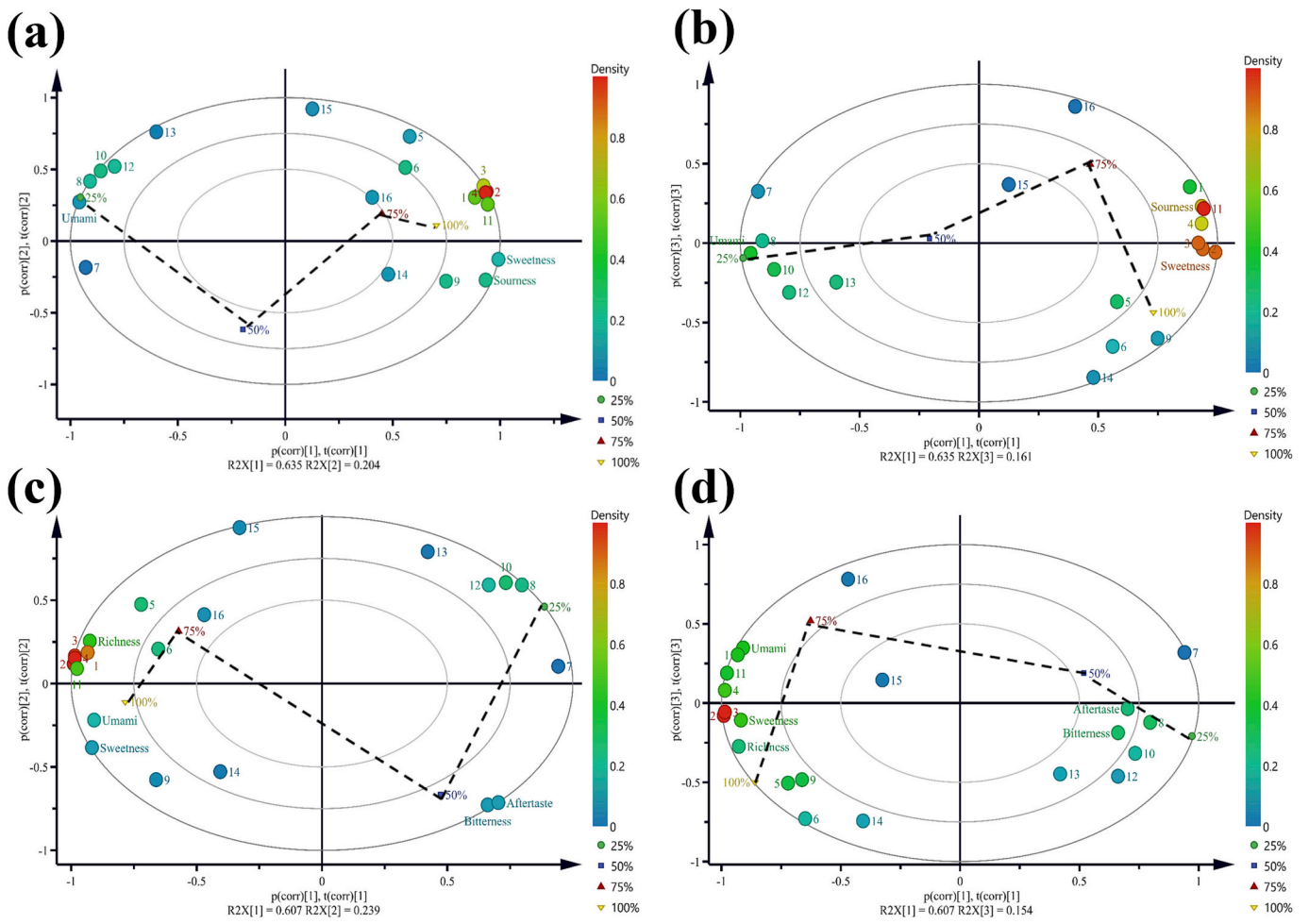

Fig. 2. The correlation matrix of the taste compounds to the taste perception during chewing (a and b was TDS taste perception, c and d was electronic tongue taste perception).

of the first principal component. At 75 % and 100 % stages of oral mastication, food clusters were located on the positive axis of the first principal component, and both sour and sweet perception were located on the positive axis of the first principal component. The results indicated that the flavor perception intensity of japonica rice was enhanced gradually with the progress of oral processing. The sour taste and sweet taste were located in the negative axis of the second principal component, and the umami flavor was located in the positive axis of the second main component. This result indicated that the umami flavor at the 25 % stage of oral chewing was stronger than that at the 75 % and 100 % stages of oral chewing, and the sweetness at the 100 % stage of oral processing was the strongest. These results are consistent with those of D-QDA.

According to the first principal component results, glucose, sucrose, proline, maltose, fructose, tartaric acid, succinic acid, glycine, histidine, arginine, and methionine were positively correlated with the perception of sweet and sour taste, among which glucose, sucrose, and proline had the greatest influence on the perception of sweet and sour taste. Aspartic acid, glutamic acid, alanine, valine, and lysine were negatively associated with the perception of sweet and sour tastes. The VIP values of 8 taste substances (glucose, sucrose, proline, maltose, fructose, succinic acid, aspartic acid, and glutamic acid) were all greater than 1 among the three principal components, indicating that these 8 compounds were significantly correlated with the perception of sweetness, umami, and sour taste during oral processing of japonica rice. As shown in Fig. 2, glucose, sucrose, proline, maltose, fructose and succinic acid have a significant positive correlation with a sweet and sour taste. In contrast, aspartic acid and glutamic acid correlate significantly negatively with a sweet and sour taste. Aspartic acid and glutamic acid were positively correlated with umami.

3.7.2. *Addition experiment*

The experimental results are shown in Table S-4. Maltose, fructose, and proline can enhance the sweetness and inhibit the intensity of umami and sour taste. Succinic acid can enhance the sour taste and inhibit sweet intensity; the results showed that glucose and sucrose significantly improved the sweetness and reduced japonica rice's sour taste. Succinic acid can substantially enhance the sour taste and reduce the sweetness of japonica rice. Therefore, glucose, sucrose, and succinic acid are the key taste substances in the oral processing of japonica rice. This result is consistent with that of Pu dandan (Pu, 2020).

3.8. *The perceptual mechanism of sweet substances*

3.8.1. *Homologous modeling of sweet taste receptor proteins T1R2/T1R3*

T1R2/T1R3 is a G-protein-coupled receptor family of taste receptors. When taste substances (ligands) bind to taste receptors, they stimulate taste receptors to produce taste perception. Since the crystal structure of T1R2/T1R3 has not been analyzed, the structure model of human T1R2/T1R3 heterodimer was constructed by SWISS-MODEL homology modeling based on the amino acid sequences of extracellular Venus flytrap domains of human T1R2 and T1R3. When homology reaches 30 %, reasonable three-dimensional structure models of proteins can be predicted (Pu, 2020). The homology modeling results of sweet taste

receptor protein T1R2/T1R3 are shown in Fig. 3a, with the homology reaching 33.3 %. Therefore, this model is reliable.

The model obtained above was evaluated through the pull diagram, and the results are shown in Fig. 3b. When the allowed region reaches more than 90 %, it indicates that the model of the homologous model is reasonable (Yu, 2019). The area between gray and green represents the reasonable area, and the area within green represents the suitable area. The results show that amino acid residues in the allowed area account

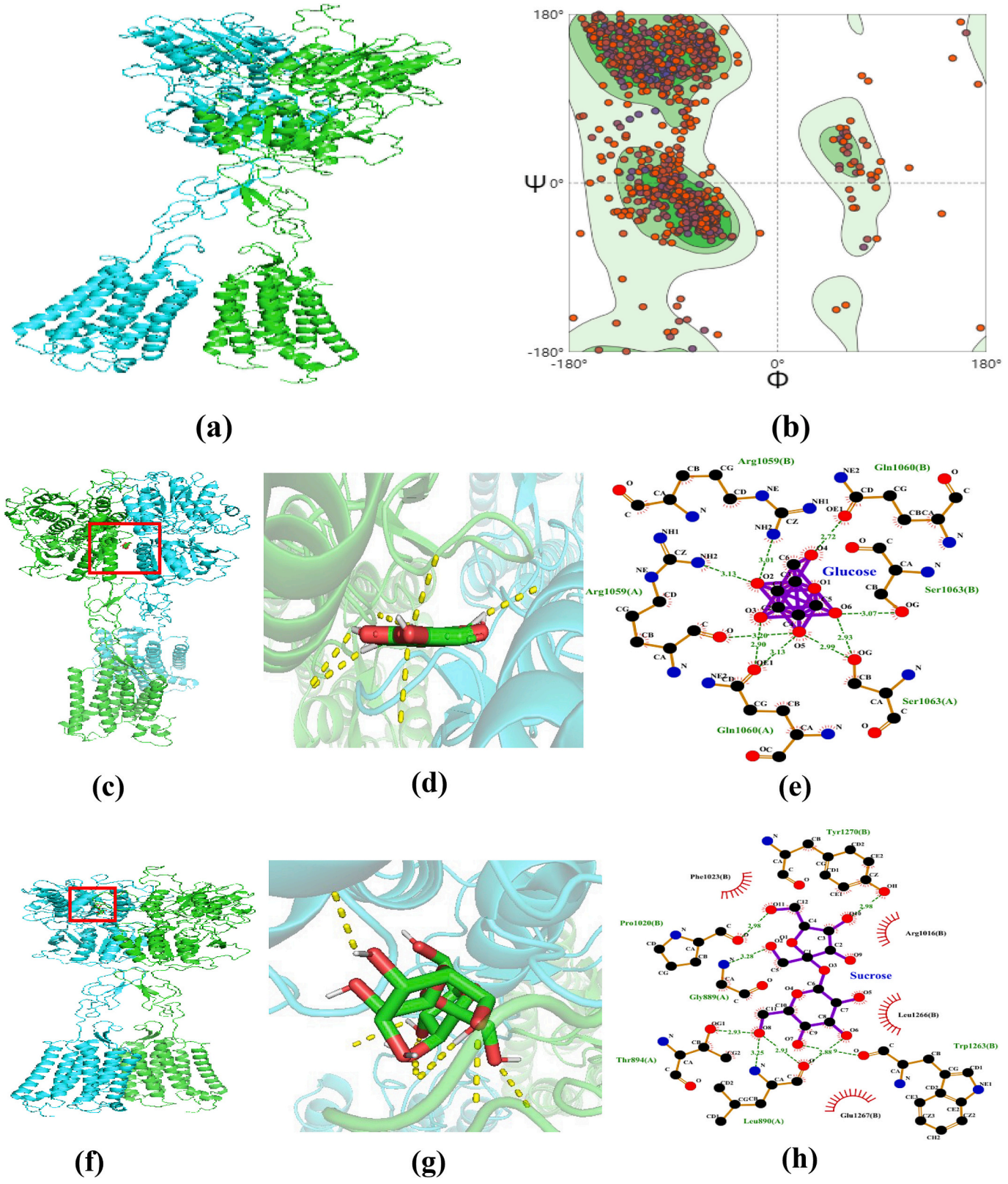

Fig. 3. Homology model and molecular docking poses of two sweet substence with T1R2/T1R3 receptor. a: Structure of sweet receptor T1R2/T1R3; b: Ramachandran plot for the T1R2/T1R3 homology model. Molecular docking results of sweet receptor T1R2 / T1R3 with glucose (a-c) and sucrose (d-f).

for 96.29 %, and those in the disallowed area account for 3.71 %. Therefore, according to the 90 % critical principle, The model constructed by homologous simulation is reasonable regarding dihedral distribution and stereoscopic collision.

3.8.2. The taste substance docked with molecules of the sweet taste receptor protein T1R2/T1R3

The affinity, force, and binding sites of sweet taste receptor protein T1R2/T1R3 for docking with 16 key taste substances are shown in Table S-5. The affinity of glucose, sucrose, and maltose was −7.7 kcal/mol, −7.5 kcal/mol, and − 7.2 kcal/mol, respectively. The lower the affinity, the more stable the ligand binds to the receptor (Yu, 2019). It is known that glucose, sucrose, and maltose bind to the taste receptor protein T1R2/T1R3 to form a stable complex, stimulating sweet taste channels and developing sweet taste perception. In addition, the affinity of sweet fructose, glycine, alanine, and proline were − 5.8 kcal/mol, −3.9 kcal/mol, −4.3 kcal/mol, and − 5.0 kcal/mol, respectively. Hydrogen bonds play a key catalytic role in stabilizing acceptor-ligand interactions, and the more hydrogen bonds, the stronger the stability (Tuersuntuoheti, 2021). As can be seen from Table S-5, fructose combines with T1R2/T1R3 to form 8 hydrogen bonds and 2 hydrophobic bonds. Glycine binds to T1R2/T1R3 to form seven hydrogen and hydrophobic bonds. Alanine binds to T1R2/T1R3 to form 7 hydrogen bonds and 5 hydrophobic bonds. Proline binds to T1R2/T1R3 to form 5 hydrogen bonds and 5 hydrophobic bonds. This may be why fructose, glycine, alanine, and proline have a lower binding affinity with T1R2/T1R3 than glucose, sucrose, and maltose. In Chapter 5, the experimental results showed that glucose and sucrose played a key role in the perception of sweetness during the oral processing of japonica rice. Therefore, the molecular conformation and binding sites of glucose and sucrose binding to sweet receptor proteins T1R2/T1R3 were used to explore the mechanism of sweet perception in japonica rice.

3.8.3. Mechanisms of sweetness perception

The docking results of glucose and sucrose with sweet taste receptor protein T1R2/T1R3 are shown in Fig. 3. As can be seen from Fig. 3 c-e, glucose combines with amino acid residues of T1R2/T1R3 to form 9 hydrogen bonds, and the hydrogen bond binding sites on the T1R2 chain are Ser1063, Arg1059, and Gln1060, respectively. The hydrogen bond length is 2.93 A, 2.99 A, 3.2 A, 3.13 A, 3.13 A and 2.9 A, respectively. The hydrogen binding sites on the T1R3 chain were Ser1063, Gln1060, and Arg1059, respectively. The hydrogen bond length is 3.07 A, 2.72 A, and 3.01 A, respectively. When the receptor and ligand bind, a hydrogen bond force is formed. The more hydrogen bonds there are, the shorter the bond length is, and the better the binding between the receptor (taste receptor) and ligand (taste substance) will be (Tuersuntuoheti, 2021). Thus, when glucose binds to amino acid residues of T1R2/T1R3, Ser1063 on the T1R2 chain is the main amino acid residue in glucose sweetness perception.

As shown in Fig. 3 f-h, sucrose binds with amino acid residues of T1R2/T1R3 to form 7 hydrogen bonds and 4 hydrophobic bonds. The hydrogen bond binding sites on the T1R2 chain are Gly889, Thr894, and Leu890, respectively. The hydrogen bond lengths were 3.2 A, 2.93 A, 3.25 A, 2.91 A and 2.88 A, respectively. The hydrogen binding sites of T1R3 were Tyr1270, Pro1020, and Trp1263, respectively. The hydrogen bond lengths were 2.98 A, 2.98 A, and 2.9 A, respectively. The hydrophobic binding sites on the T1R3 chain were Arg1016, Leu1266, Glu1267, and Phe1023, respectively. When sucrose binds with T1R2/T1R3 amino acid residues, the Leu890 amino acid residue on the T1R2 chain forms three hydrogen bonds. Therefore, Leu890 on the T1R2 chain is the most important amino acid residue in sucrose sweetness sensing. In conclusion, Ser1063 on the T1R2 chain is the main amino acid residue in glucose sweetness perception, and Leu890 on the T1R2 chain is the most important amino acid residue in sucrose sweetness perception. Glucose and sucrose bind to amino acid residues of T1R2/T1R3 mainly through hydrogen and hydrophobic bonding, resulting in increased activity of T1R2/T1R3, thus sensing sweetness.

3.9. The perceptual mechanism of umami substances

3.9.1. Homologous modeling of umami receptor proteins T1R1/T1R3

T1R1/T1R3 is a taste receptor of the G protein-coupled receptor family. Since the crystal structure of T1R1/T1R3 has not been analyzed, the structure model of the human T1R1/T1R3 heterodimer was constructed using the homology modeling method. When homology reaches 30 %, reasonable three-dimensional structure models of proteins can be predicted (Pu, 2020). The homology modeling results of umami receptor protein T1R1/T1R3 are shown in Fig. 4a-b, with the homology reaching 33.5 %. Therefore, this model is reliable. In addition, it can be seen from Fig. 4a that the structure of region A is similar to that of the Venus flytrap. Hinges connect the two leaves, and the two leaves and hinges together form a cavity. This model is consistent with the results of Yu Xiaqin (Yu, 2019).

According to the method described in 3.8.1, the model obtained above is evaluated through the pull diagram, and the results are shown in Fig. 4b. Amino acid residues in the allowable region accounted for 96.19 %, and those in the disallowed area accounted for 3.81 %. Therefore, according to the 90 % critical principle, the homology simulation model was reasonable regarding dihedral distribution and stereoscopic collisions.

3.9.2. The flavor substance docked with the umami receptor protein T1R1/T1R3

The affinity, force, and binding sites of the interaction between umami receptor protein T1R1/T1R3 and 16 key taste s**ubst**ances are shown in Table S-6. The affinity of glucose, sucrose, and maltose was −6.5 kcal/mol, −6.4 kcal/mol, and − 6.8 kcal/mol, respectively. Thus, glucose, sucrose, and maltose bind to the flavor receptor proteins T1R1/T1R3 to form a stable complex that stimulates umami formation channels and affects perception. It follows that glucose, sucrose, and maltose bind to sweet receptor proteins and umami receptor proteins. This may have to do with the interaction of sweet and umami receptors. In addition, the affinity of the umami aspartic acid and glutamate to the umami receptor protein T1R1/T1R3 was −5.8 kcal/mol- and − 5.0 kcal/mol, respectively. Aspartic acid binds to T1R1/T1R3 to form 9 hydrogen bonds and 4 hydrophobic bonds. Glutamic acid binds to T1R1/T1R3, forming five hydrogen and four hydrophobic bonds. In Chapter 5, the experimental results showed that aspartic acid and glutamic acid played a key role in the perception of umami during the oral processing of japonica rice. Therefore, the molecular conformation and binding sites of aspartic acid and glutamic acid binding to umami receptor protein T1R1/T1R3 were used to explore the japonica rice umami perception mechanism.

3.9.3. The mechanism of umami perception

The molecular docking results of aspartic acid and glutamic acid with umami receptor protein T1R1/T1R3 are shown in Fig. 4. As shown in Fig. 4c-e, aspartic acid combines with amino acid residues of T1R1/T1R3 to form 9 hydrogen bonds and 4 hydrophobic bonds. The hydrogen binding sites on the T1R1 chain were Gln1230, Gly1009, Ser1011, Ser988, and His986, respectively. The hydrogen bond length is 3.16 A, 2.96 A, 3.03 A, 3.00 A, 2.94 A, 2.97 A, 2.96 A, 2.93 A, and 3.02 A, respectively. The hydrophobic binding sites on the T1R1 chain were Ala1143, Ala1010, Ser987, and Tyr1059, respectively. When aspartic acid is combined with the amino acid residue of T1R1/T1R3, the Ser1011 amino acid residue on the T1R1 chain forms three hydrogen bonds.

As seen from Fig. 4f-h, glutamic acid binds with amino acid residues of T1R1/T1R3 to form 5 hydrogen bonds. Ser1011 on the T1R1 chain is the most important amino acid residue for aspartic acid and 4 hydrophobic bonds. The hydrogen bond binding sites on the T1R1 chain are Glu889, Arg897, and Ser900, and their hydrogen bond lengths are 3.02

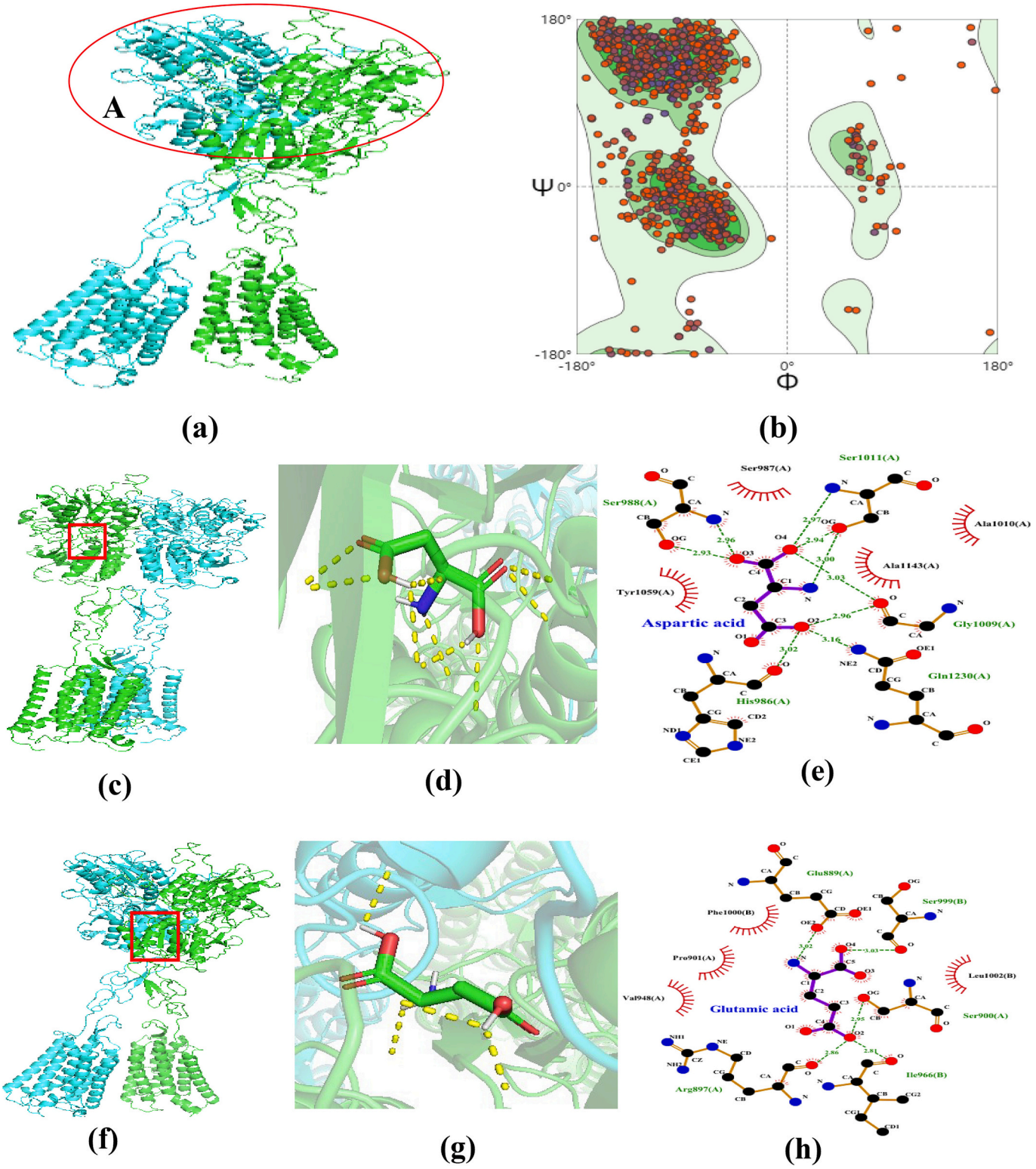

Fig. 4. Homology model and molecular docking poses of two umami substance with T1R1/T1R3 receptor. a: Structure of sweet receptor T1R1/T1R3; b: Ramachandran plot for the T1R2/T1R3 homology model. Molecular docking results of sweet receptor T1R1 / T1R3 with aspartic acid (a-c) and glutamic acid (d-f).

A, 2.86 A, and 2.95 A, respectively. The hydrophobic binding sites on the T1R1 chain were Pro901 and Val948, respectively. The hydrogen binding sites on the T1R3 chain were Ile966 and Ser999, respectively. The hydrogen bond lengths were 2.81 A and 3.03 A, respectively. The hydrophobic binding sites on the T1R3 chain were Leu1002 and Phe1000. When glutamic acid binds with T1R1/T1R3 amino acid residues, Ile966 residues on the T1R3 chain form the shortest hydrogen bond length. Therefore, Ile966 on the T1R3 chain is glutamic acid taste perception's most important amino acid residue. In conclusion, T1R1 chain Ser1011 aspartic acid taste perception is the main amino acid residues, T1R3 Ile966 is glutamic acid taste perception on the chain when the main amino acid residues. Aspartic acid and glutamate bind to

amino acid residues of T1R1/T1R3 mainly through hydrogen and hydrophobic bonding, resulting in increased activity of T1R1/T1R3, thus sensing umami.

4. Conclusion

This study examines the alterations in taste and perception mechanisms of japonica rice during oral processing. Through simulated chewing experiments and electronic tongue analysis, it was observed that soluble sugars, organic acids, flavor nucleotides, and free amino acids undergo taste substance changes during japonica rice oral processing, significantly influencing taste perception. By exploring the relationship between taste substances and sensory properties via flavor receptor protein modeling and molecular docking methods, it was revealed that glucose and sucrose interact with the sweetness receptor T1R2/T1R3 through hydrogen and hydrophobic bonding forces, enhancing sweetness perception. Aspartate and glutamic acid bind to the umami receptor T1R1/T1R3, increasing umami perception through similar bonding forces. These molecular-level insights may advance food science by enabling precision modulation of rice flavor profiles through targeted compound-receptor interactions, while offering a biochemical basis for optimizing oral processing parameters in product design. The interaction mechanisms identified between sweet and savory substances and receptor proteins offer a deeper understanding of japonica rice's taste changes and perception mechanisms during oral processing, paving the way for innovative approaches in food technology and product development. In addition , these mechanistic insights may support the creation of interactive tools that visualize how mastication-triggered molecular interactions shape taste experiences, fostering science-based dietary decision-making.

This study focused only on japonica rice and analyzed specific flavor substances. In the future, we will explore the different rice varieties and additional taste compounds that affect taste perception mechanisms and investigate the influence of cooking methods on flavor changes during oral processing. Additionally, studying the role of other sensory properties beyond taste, such as aroma and texture, in conjunction with taste substances could provide a more comprehensive understanding of how consumers experience rice consumption.

Author contribution

Sailimmuhan Asimi designed the experiment, analyzed the experimental data, and wrote the manuscript. Prof. Zhang Min was the research leader, supervised the project, and revised the manuscript.

The colors in the figure range from red to blue, representing the contribution of the corresponding flavor substance. The numbers in the figure represent taste substances with TAV values greater than 1:1: fructose, 2: glucose, 3: sucrose, 4: maltose, 5: tartaric acid, 6: succinic acid, 7: aspartic acid, 8: glutamic acid, 9: glycine, 10: alanine, 11: proline, 12: valine, 13: lysine, 14: histidine, 15: arginine, 16: Methionine.

CRediT authorship contribution statement

Sailimuhan Asimi: Writing – review & editing, Writing – original draft, Investigation, Formal analysis. **Zhang Min:** Writing – review & editing, Resources, Funding acquisition.

Declaration of competing interest

The authors declare that they have no known competing financial interests or personal relationships that could have appeared to influence the work reported in this paper.

Acknowledgments

This study was supported by the Discipline of Construction-Food Science and Engineering [SPKX-202202]. Xinjiang Uygur Autonomous Region 2022 "Tianchi Talent" Introduction Program Youth Doctoral Program. The 14-th Five-Year Plan Distinctive Program of Public Health and Preventive Medicine in Higher Education Institutions of Xinjiang Uygur Autonomous Region. In addition, our native English speaker colleague Amjad Sohail helped revise the English grammar in the manuscript. We sincerely thank him for his help.

Appendix A. Supplementary data

Supplementary data to this article can be found online at https://doi.org/10.1016/j.fochx.2025.102427.

Data availability

No data was used for the research described in the article.

References

Asimi, S., Ren, X., Zhang, M., et al. (2021). Establishment of an oral processing model for three varieties of rice. *Journal of Food Processing and Preservation, 45*(11), Article e15920.

Asimi, S., Ren, X., Zhang, M., et al. (2022a). Characterization of japonica rice aroma profiles during in vitro mastication by gas chromatography-ion mobility spectrometry (GC-IMS) and electronic nose technology. *International Journal of Food Engineering, 18*(10–11), 679–688.

Asimi, S., Ren, X., Zhang, M., et al. (2022b). Effect of oral processing on texture, rheology properties, and microstructure of three rice varieties. *Journal of Food Process Engineering, 45*(2), Article e13982.

Asimi, S., Xin, R., Min, Z., et al. (2022). In vitro mastication of cooked rice: How it influences the bolus characteristics. *Journal of Food Process Engineering, 45*(1), Article e13945.

Chen, H., Yang, G., Xiao, Y., et al. (2023). Effects of nitrogen and phosphorus fertilizer on the eating quality of indica rice with different amylose content[J]. *Journal of Food Composition and Analysis, 2023*. https://doi.org/10.1016/j.jfca.2023.105167

Chen, J. (2015). Food oral processing: Mechanisms and implications of food oral destruction. *Trends in Food Science and Technology, 45*(2), 222–228.

China, S. A. O. T. P. S. R. O. (2016). Determination of fructose, glucose, sucrose, maltose, and lactose in food. In *High-Performance Liquid Chromatography*. Beijing: China Standards Press.

Dandan, P. (2020). *Sensory perception for bread oral processing and the mechanisms of saliva* (Ph.D. dissertation,. Beijing: China Agricultural University.

Dandan, P., Huiying, Z., Yuyu, Z., et al. (2019). Characterization of the oral breakdown, sensory properties, and volatile release during mastication of white bread. *Food Chemistry, 298*, Article 119878.

Dandan, P., Zhang, Y., Sun, B., et al. (2020). Characterization of the key taste compounds during bread oral processing by instrumental analysis and dynamic sensory evaluation. *LWT - Food Science and Technology, 138*, Article 110641.

Deng, Y. (2017). *Effect of oral processing on mouthfeel quality of Chinese traditional stewed pork with brown sauce* (Master's thesis,. Nanjing: Bohai University.

Dengyong, L., & Zhenxia, C. (2020). Aroma release from stewed pork with brown sauce during oral processing. *Food Science, 41*(4), 123–130.

Dongxiao, L. (2021). *Study on the eating and tasting characteristics of Indica rice during oral processing* (Master's thesis,. Beijing: Beijing Technology and Business University.

Lapis, T. J., Penner, M. H., & Lim, J. (2016). Humans can taste glucose oligomers independent of the hT1R2/hT1R3 sweet taste receptor. *Chemical Senses, 41*(9), 755–762.

Liu, H., Da, L. T., & Liu, Y. (2019). Understanding the molecular mechanism of umami recognition by T1R1-T1R3 using molecular dynamics simulations. *Biochemical and Biophysical Research Communications, 514*(3), 967–973.

Mandel, A. L., & Breslin, P. A. S. (2012). High endogenous salivary amylase activity is associated with improved glycemic homeostasis following starch ingestion in adults. *The Journal of Nutrition, 142*(3), 440–445.

Nelson, G., Hoon, M. A., Chandrashekar, J., et al. (2001). *Mammalian sweet taste receptors. CELL, 106*(3), 381–390.

Nguyen, P. T. M., Bhandari, B., & Prakash, S. (2016). Tribological method to measure lubricating properties of dairy products. *Journal of Food Engineering, 168*, 27–34.

Oliver, P., Cicerale, S., Pang, E., & Keast, R. (2018). A comparison of temporal dominance of sensation (TSD) and quantitative descriptive analysis (DQD) to identify flavors in strawberries. *Journal of Food Science, 83*(4), 1094–1102.

Ong, M. H., & Blanshard, J. M. V. (1995). Texture determinants in cooked, parboiled rice. I: Rice starch amylose and the fine structure of amylopectin. *Journal of Cereal Science, 21*(3), 251–260.

Pionnier, E., Cha Ba Net, C., Mioche, L., et al. (2004). In vivo nonvolatile release during eating of a model cheese: Relationships with oral parameters. *Journal of Agricultural and Food Chemistry, 52*(3), 565–571.

Saint-Eve, A., Panouillé, M., Capitaine, C., et al. (2015). Dynamic aspects of texture perception during cheese consumption and relationship with bolus properties. *Food Hydrocolloids, 46*, 144–152.

Salles, C., Chagnon, M. C., Feron, G., et al. (2011). In-mouth mechanisms leading to flavor release and perception. *Critical Reviews in Food Science and Nutrition, 51*(1), 67–90.

Shiozawa, K., Kohyama, K., & Yanagisawa, K. (2010). Changes in physical properties of a bolus during mastication of cooked rice. *Journal Of Mastication And Health Society, 15* (1), 37–42.

Stokes, J. R., Boehm, M. W., & Baier, S. K. (2013). Oral processing, texture and mouthfeel: From rheology to tribology and beyond. *Current Opinion in Colloid & Interface Science, 18*(4), 349–359.

Tuersuntuoheti, T. (2021). *Study on the quality changes of Qingke barley fresh noodles and bioactive mechanism of Qingke barley polyphenols* (Ph.D. dissertation,. Beijing: Beijing Technology and Business University.

Yu, X. (2019). *Structural simulation of umami receptor T1R1/T1R3 and the interaction with umami hexapeptides* (Master's thesis,. Shanghai: Shanghai Ocean University.

Zhu, L., Cheng, L., Zhang, H., et al. (2019). Research on migration path and structuring role of water in rice grain during soaking. *Food Hydrocolloids, 92*, 41–50.